

# Heschl's Gyrus, Posterior Superior Temporal Gyrus, and Mid-Ventrolateral Prefrontal Cortex Have

## Different Roles in the Detection of Acoustic Changes

Marc Schönwiesner, Nikolai Novitski, Satu Pakarinen, Synnöve Carlson, Mari Tervaniemi and Risto Näätänen

*J Neurophysiol* 97:2075-2082, 2007. First published Dec 20, 2006; doi:10.1152/jn.01083.2006

**You might find this additional information useful...**

---

This article cites 51 articles, 11 of which you can access free at:

<http://jn.physiology.org/cgi/content/full/97/3/2075#BIBL>

Updated information and services including high-resolution figures, can be found at:

<http://jn.physiology.org/cgi/content/full/97/3/2075>

Additional material and information about *Journal of Neurophysiology* can be found at:

<http://www.the-aps.org/publications/jn>

---

This information is current as of March 29, 2007 .

# Heschl's Gyrus, Posterior Superior Temporal Gyrus, and Mid-Ventrolateral Prefrontal Cortex Have Different Roles in the Detection of Acoustic Changes

Marc Schönwiesner,<sup>1,2,5</sup> Nikolai Novitski,<sup>1,2</sup> Satu Pakarinen,<sup>1,2</sup> Synnöve Carlson,<sup>2,3,4</sup> Mari Tervaniemi,<sup>1,2</sup> and Risto Näätänen<sup>1,2</sup>

<sup>1</sup>Cognitive Brain Research Unit, Department of Psychology, <sup>2</sup>Helsinki Brain Research Centre, and <sup>3</sup>Neuroscience Unit, Institute of Biomedicine/Physiology, University of Helsinki, Helsinki, Finland; and <sup>4</sup>Medical School, University of Tampere, Tampere, Finland; and <sup>5</sup>Advanced Magnetic Imaging Centre, Helsinki University of Technology, Finland

Submitted 10 October 2006; accepted in final form 20 December 2006

**Schönwiesner M, Novitski N, Pakarinen S, Carlson S, Tervaniemi M, Näätänen R.** Heschl's gyrus, posterior superior temporal gyrus, and mid-ventrolateral prefrontal cortex have different roles in the detection of acoustic changes. *J Neurophysiol* 97: 2075–2082, 2007. First published January 3, 2007; doi:10.1152/jn.01083.2006. A part of the auditory system automatically detects changes in the acoustic environment. This preattentive process has been studied extensively, yet its cerebral origins have not been determined with sufficient accuracy to allow comparison to established anatomical and functional parcellations. Here we used event-related functional MRI and EEG in a parametric experimental design to determine the cortical areas in individual brains that participate in the detection of acoustic changes. Our results suggest that automatic change processing consists of at least three stages: initial detection in the primary auditory cortex, detailed analysis in the posterior superior temporal gyrus and planum temporale, and judgment of sufficient novelty for the allocation of attentional resources in the mid-ventrolateral prefrontal cortex.

## INTRODUCTION

Detecting changes in the environment is essential for the survival of many organisms. Brain mechanisms of acoustic change detection have been extensively studied in humans using EEG. The prime experimental model of auditory change detection is the presentation of infrequent deviant events in a stream of repeating standard events. The deviant sounds evoke a frontal negative deflection in the auditory event-related potential, the mismatch negativity (MMN) (Näätänen et al. 1978). The MMN can be recorded in response to any discriminable change in the stimulus stream, and the response amplitude correlates with the magnitude of the acoustic change. The MMN is important in two respects: first as a means to study the mechanisms of change detection and how these relate to other cognitive processes such as attention and memory and second as a widely used tool in diverse areas of research, including language acquisition, sound localization, and psychiatric and developmental disorders (Näätänen 1995, 2003).

The MMN is often interpreted to imply the existence of a sensory–memory trace in which the features of the frequently occurring standard stimuli are represented. Much research has been dedicated to the translation of this psychological model into neurobiological mechanisms. The localization of the cerebral origin of the mismatch negativity potential was a major

aim in several functional MRI (fMRI), magneto-encephalographic, and high-density EEG studies. However, the regional specificity of the results has remained relatively low. Two contributions to the change response, one from the temporal lobes and one from the right frontal lobe, were suggested on the basis of the current density distribution of evoked potentials (Giard et al. 1990) and reductions of the MMN amplitude in patients with lesions in the frontal and temporal lobes (Alain et al. 1998; Alho et al. 1994). Since then, a number of neuroimaging studies have tried to locate the generators of these components (Doeller et al. 2003; Liebenthal et al. 2003; Marco-Pallares et al. 2005; Mathiak et al. 2002; Molholm et al. 2005; Muller et al. 2002; Opitz et al. 1999; Rinne et al. 2005; Schall et al. 2003; Tervaniemi et al. 2006). Results vary substantially across these experiments. Nevertheless, all of these studies report activation in the region of the superior temporal gyrus, sometimes including Heschl's gyrus, and several found activation of the inferior frontal gyrus.

A more precise localization that allows reliable comparison to known anatomical areas or functional parcellations of the superior temporal and inferior frontal gyri would allow significant progress in the understanding of preattentive change detection. For instance, the part of the inferior frontal gyrus in which most of the reported MMN-related activations fall can be subdivided into three areas (Brodmann areas 44 and 45 and the deep frontal operculum), with different connection patterns in individual subjects using diffusion tensor imaging (Anwander et al. 2007). A second example is the question of whether the change-detection mechanism is co-localized with primary feature processing (i.e., does the detection of small pitch changes happen in areas that extract pitch). This is a tacit, but unproven, assumption in studies that use the MMN as a tool to locate the processing of acoustic features (Pulvermüller et al. 2006; Shestakova et al. 2004; Tervaniemi et al. 2006).

Several factors have considerably hindered pinpointing the location of the change-related effects with higher regional specificity using fMRI: 1) the response to a subtle change in a stream of acoustic stimuli is much smaller in magnitude than the response to an isolated sound; 2) the dynamic range of the response is further decreased by the MRI scanner noise if images are acquired continuously; 3) in block-design experiments, the number of standard stimuli between deviants is necessarily low, decreasing the amplitude of responses to the

Address for reprint requests and other correspondence: M. Schönwiesner, Dept. of Neurology and Neurosurgery, Montreal Neurological Inst., McGill Univ., 3801 rue University, Montreal, Quebec H3A 2B4, Canada (E-mail: marc.schoenwiesner@mcgill.ca).

The costs of publication of this article were defrayed in part by the payment of page charges. The article must therefore be hereby marked "advertisement" in accordance with 18 U.S.C. Section 1734 solely to indicate this fact.

deviants (Haenschel et al. 2005); 4) responses to sounds deviating in frequency (the most commonly used deviant type) are confounded, because infrequent stimulation with a different frequency will activate “fresh” neural populations in tonotopically organized cortical areas—this is not the case for other sound features that are not represented topologically, such as violations of temporal order (complex MMN; see Paavilainen et al. 2001), and perhaps sound duration (but see Pantev et al. 1989); 5) studies using duration deviants to avoid adaptation-related confounds have not accounted for the decreased stimulus energy of deviants shorter than the standard, further diminishing the amplitude of the response. Some of the previous studies address one or more of these points, but none addresses all.

Here we surmount those problems with a parametric event-related fMRI and EEG experiment, using sparse imaging to eliminate the effects of scanner noise. This procedure permits localization of the responses in individual brains, as well as individual comparison of EEG and fMRI results. We measure responses to several deviant magnitudes to separate different parts of the change detection mechanism.

## METHODS

### Participants

Thirteen volunteers (between 20 and 30 yr, 4 male, 10 right-handed) took part in this experiment after giving written informed consent. The participants had no history of audiological or neurological disease. The experimental procedures conformed with the Code of Ethics of the World Medical Association (Declaration of Helsinki) and were approved by the Ethics Committee for Ophthalmology, Otolaryngology, Neurology, and Neurosurgery of the University Hospital and by the Ethics Committees of the Department of Psychology of the University of Helsinki.

### Stimuli

All sounds were click trains with a rate of 500 Hz, low-pass filtered at 8,000 Hz. At this rate, the clicks are not perceived individually but as a complex tone with a pitch of 500 Hz, including all harmonics of this frequency up to the low-pass filter cut-off. The number of clicks was varied to generate stimuli of different durations: 100, 74, 52, and 30 ms. The 100-ms click train is referred to as “standard,” whereas the shorter click trains are referred to as “deviants,” specifically as small (74 ms), medium (52 ms), and large deviants (30 ms), according to the acoustical difference from the standard sound. The sound durations were chosen to elicit an approximately linear increase in the magnitude of the deviance response (Näätänen et al. 2004). The stimuli were equalized for root-mean-square energy, so that the energy contour of a sequence of stimuli was constant over time. Changes in the sound duration were thus the only salient feature in the stimulus stream to elicit responses. No attempt was made to control for effects of the physical differences between standard and deviant sounds on brain activation, such as the shorter delay of the neural offset response to deviants of slightly shorter duration than standard sounds. Such effects can be controlled by reversing the role of standards and deviants between blocks (Kujala et al. 2007). Note, however, that because of its low temporal resolution, fMRI is relatively insensitive to differences in the temporal layout of the response, such as caused by the slightly different delay of the sound offset. It is therefore unlikely that this particular confound of sound duration changes is a large factor in the observed responses.

During the EEG session, scanner noise recorded from the sequence used in the fMRI experiment was played back to the participants, simulating the acoustical environment in the MRI scanner.

### Procedures

All participants took part in an EEG recording and in a subsequent fMRI session. fMRI scanning was done at the Advanced Magnetic Imaging Centre, Helsinki. During the fMRI session, participants wore pneumatic headphones (which provided sufficient playback quality for the relatively simple stimuli), and looked at a screen through a mirror attached to the head coil. Auditory stimulus presentation was organized in 9-s trials. Each trial started with the 1.2-s sound of the fMRI image acquisition, played back through headphones (in the EEG session) or produced by the scanner (in the fMRI session). Starting 50 ms past trial onset and continuing during the whole duration of the trial, 27 100-ms click trains were presented repetitively with a stimulus onset asynchrony of 333 ms. Either 2, 3, 4, 5, or 7 s before trial offset, one of the standard stimuli was replaced by a deviant sound. While irrelevant in the EEG session, this timing allowed estimation of the hemodynamic response to the deviants in the fMRI session (Fig. 1).

We weighted the sampling of the hemodynamic response function according to their potential contribution in locating the responses, i.e., we acquired most repetitions from time-points close to the expected peak of the hemodynamic response, thus trading some of the response function estimation power for response detection power. For each deviant, we acquired 15, 20, 20, 20, and 10 repetitions for time-points 2, 3, 4, 5, and 7 s, respectively (85 repetitions in total). Additionally, 25 trials containing only standard sounds served as a baseline, making up a total of 16 experimental conditions (3 deviant types  $\times$  5 possible onset times within the trial + baseline). Altogether 280 trials (85 trials per deviant  $\times$  3 deviant types + 25 baseline trials) were presented in pseudorandom order with equalized transition probabilities. Total experimental time in the fMRI session was 42 min, which was split in four runs.

To control attention and direct it away from the acoustic stimuli and to reduce eye movements, participants were asked to fixate a cross at the center of the screen and perform a visual control task. The task was to press a button with the left or right index finger on each occurrence of a capital letter in a sequence of random digits that were shown at the center of the screen. The digits were presented for 80 ms at irregular intervals with an average of four digits per trial. The target occurred on average once every two trials. After the fMRI session, participants were asked to rate their level of alertness during scanning, the subjective sound level, and the difficulty of the task in comparison to the EEG session.

During the EEG session, participants were seated in a comfortable chair in a sound attenuated room. The presentation of the experiment and the task were the same as in the fMRI session. Because the EEG analysis required a higher number of repetitions per deviant, the experiment was run twice during the EEG session.

### EEG recording and analysis

An EEG was recorded with 128 active sintered Ag-AgCl electrodes (BioSemi, Amsterdam, The Netherlands), positioned radially equidistantly.

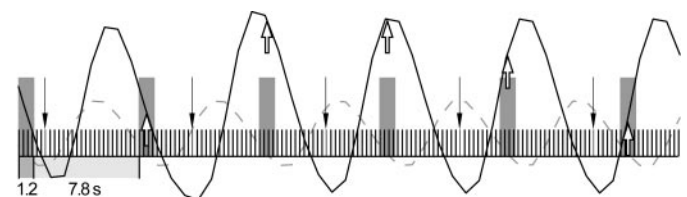


FIG. 1. Experimental design in functional MRI (fMRI) session. Image acquisition (gray bars) left 7.8 s of silence for stimulus presentation (row of black lines) and decay of response to scanner noise (dashed line). Deviant stimuli (black arrows) were presented a different time-points in relation to image acquisition. This allowed sampling of different time-points (white arrows) of hemodynamic response (black curve) at 2, 3, 4, 5, and 7 s (from right to left) after deviant onset.

tant from the vertex across the scalp (BioSemi ABC layout). Additional electrodes were placed at the left and right mastoid, at the outer canthi of each eye, at the right eye supra- and infraorbitally, and on the nose tip. The setup does not use a conventional recording reference but instead actively clamps the average potential of the subject by a feedback loop between two dedicated electrodes to the A/D conversion reference voltage. The data were recorded direct-current-coupled and digitized with 512-Hz sampling rate. Low-pass filtering to avoid aliasing was performed by the decimation filter of the A/D converter (5th order sinc response,  $-3$  dB point at 102 Hz). The resulting data files were transformed into the Neuroscan continuous data format (PolyRex software, <http://psychophysiology.cpmc.columbia.edu/Software/PolyRex>; constant gain across all data sets). Signals from the scalp electrodes were rereferenced to the nose tip potential. Signals from the face electrodes were used to compute the horizontal and vertical bipolar electro-oculogram. The data were filtered with a digital band-pass filter between 1 and 15 Hz with slopes of 24 dB/octave. Data epochs from 100 ms before to 350 ms after stimulus onset with samples exceeding  $\pm 75$   $\mu$ V were rejected from the subsequent analysis. The data were visually inspected for residual artifacts. Responses to standards (excluding standards directly after deviants) and each of the deviants were averaged separately. The responses to standards were subtracted from those to deviants. In such difference waveforms, the MMN is a negative-going potential at  $F_z$  and a positive-going potential at the right and left mastoid in the range of 150–250 ms after deviant onset. To assess statistical significance of MMN responses, the distribution across participants of peak amplitudes in the baseline interval was compared with the distribution of peak amplitudes across participants in an interval of equal length around the latency of the grand average MMN. This method was chosen instead of the usual comparison of individual peak amplitudes in the MMN latency range to zero, which is slightly biased, because the expected value of amplitude maxima in a certain time range in the absence of a signal is not zero. If this value reflects noise in the signal and the experimental conditions are presented in a balanced pseudo-random sequence, the distribution of baseline amplitude maxima across conditions should be nearly identical. A significant difference in the baseline power between deviant conditions might bias the results of a test for significance of the MMN responses. The peak amplitudes in the root mean square across all channels of the EEG data in both intervals for all participants and deviant conditions were entered into a one-tailed paired *t*-test. We also tested for equal baseline peak amplitude using a two-way ANOVA with factors interval and deviance. If the baseline power is caused by noise, a significant interaction between interval and deviant conditions is expected (effect of deviant in the MMN but not baseline interval). The peak amplitudes of the MMN responses at  $F_z$  were additionally subjected to a one-way ANOVA with factor deviance and at right and left mastoids with two-way ANOVA with factors deviance and hemisphere. Greenhouse-Geisser correction was applied when necessary.

To obtain a data-driven estimate of the number of components in the MMN response, we performed a spatial principal component analysis of the individual evoked potentials, and visualized the probable cerebral origin of the first two principal components as the average of the electrode locations weighted by the contribution of each electrode to the principal component analysis (PCA) component. This estimate takes into account that PCA components are often not dipolar. These location estimates were used solely to seed a subsequent dipole model, and all further analyses and conclusions are based on the dipole analysis.

The sources of the responses to the three different deviants were analyzed with three regional sources and a four-shell ellipsoidal volume conductor as a head model using version 5.1 of the Brain Electrical Source Analysis software (BESA, Gräefelfing, Germany). The locations of two of the regional sources were constrained to be symmetric about the midsagittal plane, and fitting was performed

within a 50-ms time window centered on the peak of the response. Within the fit window, the residual variance of the model amounted to only 1.4% for the small, 0.7% for the medium, and 1.1% for the large deviant condition.

The model was used as a spatial filter to derive the activation time-course of each regional source (source waveform) for the three deviant conditions in the grand-average and in each individual separately. The orientations of the regional sources were adjusted in each individual so that one of the components captured the maximum of the global field power in the fit window. The peak amplitudes of these components across individuals were analyzed in a two-way ANOVA with factors deviance and location. Greenhouse-Geisser correction was applied when necessary. Post hoc analyses were performed with Tukey's test for honestly significant differences.

### fMRI and analysis

Blood-oxygen level dependent contrast images were acquired at 3 T (SIGNA EXCITE, General Electric) using gradient echo planar imaging (TR/TE 9,000 ms/32 ms) with a head quadrature receiver/transmitter coil. The functional images consisted of 19 ascending slices with an in-plane resolution of  $3 \times 3$  mm (matrix size  $64^2$ ), a slice thickness of 3 mm, and an interslice gap of 1 mm. The seventh slice followed the line connecting the anterior and posterior commissures. The slices were acquired in direct temporal succession in the first 1,200 ms of the TR, followed by 7,800 ms of stimulus presentation without acquisition noise. This clustering of the slice acquisition at the beginning of a long TR (sparse imaging) reduces the effect of scanner noise on the recorded response to the stimuli (Edmister et al. 1999; Hall et al. 1999).

A high-resolution structural image was acquired from each subject using a T1-weighted spoiled grass gradient-recalled three-dimensional (3D) sequence with a resolution of  $1 \text{ mm}^3$  (matrix size,  $256 \times 256 \times 150$ ).

Data were corrected for head motion [1 participant's data were excluded from further analysis because of excessive ( $>2$  mm) head translation], spatially smoothed with a 6- (individual participant analysis) or 10-mm (group analysis) full-width-at-half-maximum Gaussian kernel, and transformed into the stereotaxic space of the international consortium for brain mapping 152 atlas (MNI space) using MINC 1.4 software. Statistical analysis was done with Matlab (The MathWorks, Natick, MA) and the FMRISTAT toolbox (Worsley et al. 2002). All deviant conditions were contrasted with the baseline condition, and regions of interest (ROIs) were defined as nine-voxel neighborhood of local maxima in the resulting statistical parameter map. Hemodynamic response functions in those ROIs were estimated by contrasting responses to each of the three deviants at each of the five time-points separately with the baseline. Because of the high number of modeled conditions, this is the statistically least powerful contrast, and only group level effects are reported. The average hemodynamic response function was used to model the responses to all three deviants in a single contrast against the baseline in individual participants. This is the statistically most powerful contrast, and resulting statistical parameter maps were used to identify activated areas in individual brains. The individual results were combined in a random effects analysis to allow inferences on population level (Worsley et al. 2002) and identify activated areas in the group. Signal changes in response to the three deviants were extracted from the ROIs to check correlation with EEG results.

## RESULTS

Significant mismatch negativity (MMN; Fig. 2) responses to the deviant sounds were observed in EEG recordings (comparison of RMS maxima in baseline and MMN intervals:  $P < 0.0001$ ;  $t_{12} > 7$  for large and medium deviants;  $P < 0.0087$ ;  $t_{12} =$

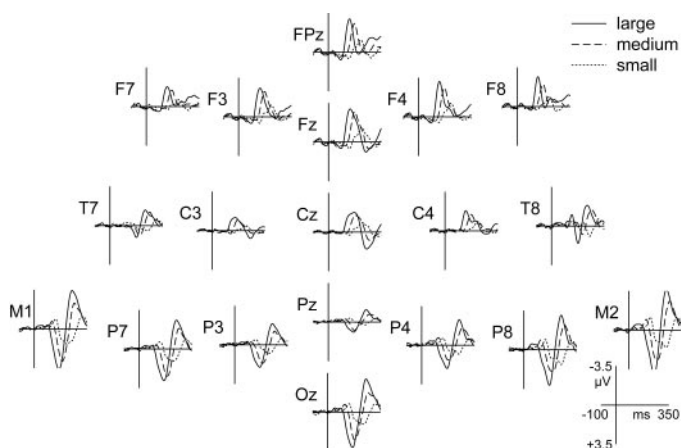


FIG. 2. Grand-average mismatch potentials in response to large, medium, and small deviants at different locations across scalp (nomenclature of locations according to extended 10–20 system; Jasper 1958; Sharbrough et al. 1991). Amplitude difference between responses to standard and deviants is plotted over time relative to stimulus onset.

2.7 for small deviant; ANOVA of RMS maxima in baseline and MMN intervals: effect of interval  $P < 0.0001$ ,  $F_{1,11} = 43.9$ , effect of deviant  $P = 0.001$ ,  $F_{2,10} = 17.4$ , interaction interval  $\times$  deviant  $P < 0.0001$ ,  $F_{2,10} = 22.6$ , no significant differences in baseline RMS maxima across deviant conditions). MMN amplitudes at  $F_z$  and at the mastoids increased with deviance magnitude (ANOVA of voltage maxima:  $P < 0.001$ ;  $F_z$ :  $F_{2,24} = 15.8$ , mastoids:  $F_{2,26} = 30.6$ ). There was no significant effect of the factor hemisphere. The latency of the MMN decreased with deviance magnitude ( $P < 0.05$ ;  $F_z$ :  $F_{2,24} = 4.3$ , mastoids:  $F_{2,26} = 4.3$ ).

No differences were observed between the reaction times and detection rates for the visual target detection task between the fMRI and EEG sessions. Most participants reported a similar subjective difficulty of the task in both sessions, but three subjects reported that the novel environment of the MR scanner made it initially more difficult to concentrate.

We performed a random effects analysis of the groups' fMRI data to localize cerebral origins of these responses. Clusters of significant ( $P < 0.05$  corrected) activations were found bilaterally in the temporal lobes and in the right inferior frontal lobe (Fig. 3).

The anatomical loci of the activation maxima were as follows (see Table 1 for coordinates): medial and lateral Heschl's gyri (HG), antero-lateral and medial portions of the left planum temporale (PT), portions of the superior temporal gyrus (STG) and sulcus (STS) inferior and posterior to HG, and the mid-ventrolateral prefrontal cortex, bracketed by the horizontal and ascending rami of the inferior frontal sulcus (Brodmann area 45). Hemodynamic responses in those areas peaked  $\sim 3$ – $4$  s after deviant onset and returned to baseline  $\sim 7$  s after deviant onset (Fig. 4, top).

A hemodynamic response function was fitted to the average of all responses and used to model the response magnitude for each deviant across the five time-points. In activated areas of the superior temporal lobe, but not in the prefrontal cortex, the response magnitude increased with the deviance magnitude (Fig. 4, bottom).

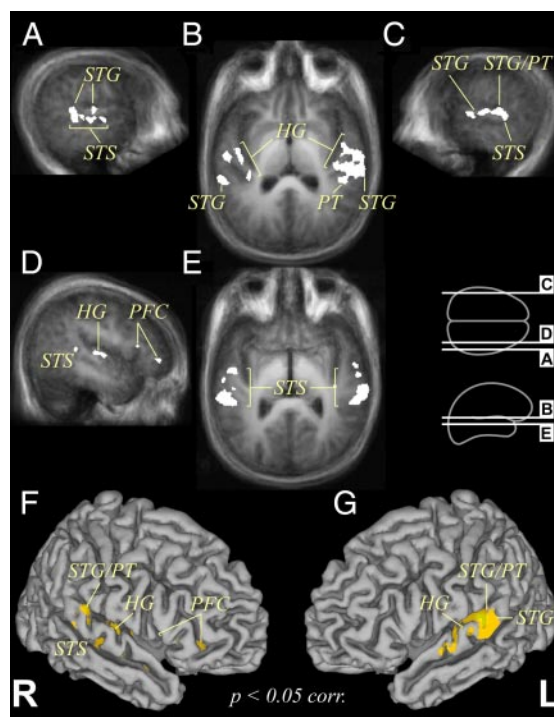


FIG. 3. Activations in response to duration changes. Statistical parameter maps showing significant responses ( $P < 0.05$  corrected) shown on sections through mean structural image of group (A–E: radiological orientation; inset: slice locations) and on an individual gray matter surface [international consortium for brain mapping single subject anatomical template; right (F) and left hemispheres (G)]. HG, Heschl's gyrus; STG, superior temporal gyrus; PT, planum temporale; STS, superior temporal sulcus; PFC, mid-ventrolateral prefrontal cortex.

### Results of individual participants

To check the consistency of the group results across individuals, statistical parameter maps were computed for each participant. Activated areas were compared with individual structural images, and effect sizes were extracted from local maxima in the maps. The constant stream of standard stimuli

TABLE 1. Brain areas activated by duration changes in the acoustic stimulus stream

Region	Side	Coordinates (x,y,z)	t	P
HG				
Medial	L	–44, –25, 7	6.9	<0.001
Lateral	L	–52, –12, –1	6.4	<0.001
Medial	R	42, –20, 5	6.4	<0.001
Lateral	R	46, –10, 1	5.6	0.003
PT	L	–50, –35, 16	6.1	<0.001
STG	L	–63, –28, 10	8.2	<0.001
	R	65, –36, 6	5.7	0.002
STS				
Middle	L	–64, –16, –2	6.2	<0.001
Anterior	L	–62, –2, –8	6.8	<0.001
	R	60, –23, –4	5.3	0.001
IFG				
Ascending ramus	R	46, 23, 11	4.9	0.041
Horizontal ramus	R	49, 32, 2	5.0	0.028

Coordinates are in MNI space (lookup available at [www.bic.mni.mcgill.ca/cgi/icbm\\_view](http://www.bic.mni.mcgill.ca/cgi/icbm_view)).  $P$  values are corrected for multiple comparisons. HG, Heschl's gyrus; PT, planum temporale; STG, superior temporal gyrus; STS, superior temporal sulcus; IFG, inferior frontal gyrus.

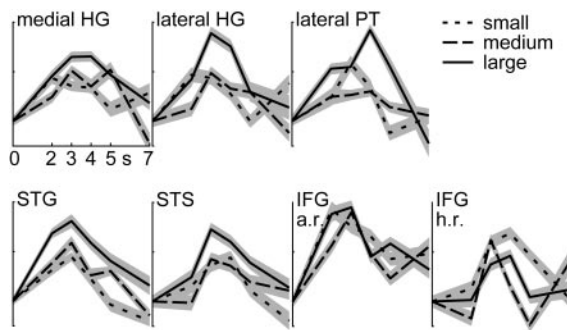


FIG. 4. Hemodynamic responses from different cerebral locations to small, medium, and large deviants (arbitrary units). IFG a.r./h.r., ascending and horizontal rami of inferior frontal gyrus, respectively.

reduces the dynamic range of responses to deviant stimuli compared with typical sound versus silence contrasts. Responses were nevertheless clear in all participants, albeit with a high degree of interindividual variability (Fig. 5).

Note that while the locations of the suprathreshold local maxima were variable, the regions that show responses just-below threshold were similar in all participants (leading to significant activations in the random effects analysis). The majority of the activation foci in the superior parts of the temporal lobes were in HG, STG, STS, and PT. The small foci in the frontal lobes were consistently located in parts of the mid-ventrolateral prefrontal cortex across subjects.

To compare the responses from temporal and frontal sites between fMRI and EEG sessions, we separated the individual ERPs into temporal and frontal components using source analysis. To check whether this separation is in fact possible in a data-driven manner without knowledge of the fMRI activa-

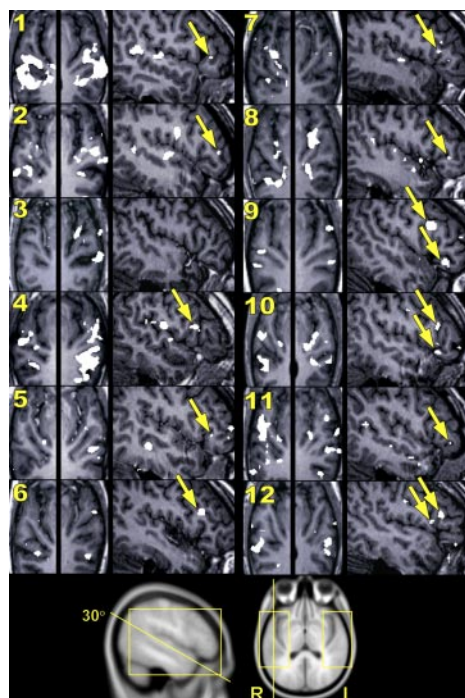


FIG. 5. Individual activation patterns (radiological orientation, position, and extent of slice portions indicated at bottom). Responses in superior temporal lobes showed considerable variation across the 12 participants. Responses in frontal lobes (arrows) clustered consistently around the horizontal and ascending rami of the IFG.

tion sites, we performed a spatial PCA of the individual ERPs. In all individuals, the first component was localized between the superior parts of the left and right temporal lobes, consistent with a superposition of bilateral responses from the auditory cortices. The second component was located in the inferior part of the frontal lobe in the majority of individuals, with a slight average lateralization to the right. The locations of these two components indeed suggested temporal and frontal contributions to the overall response, consistent with the hemodynamic response pattern.

To obtain a reliable estimate of the response of the temporal and frontal contributions to the different deviant sounds, we analyzed the sources of the evoked potentials with equivalent current dipole modeling, using the location estimates of the principal components as seeds. The group average responses were modeled with three regional sources, two of them with a symmetry constraint to account for bilateral responses from the auditory cortices. The resulting sources were located bilaterally in the vicinity of HG and in the right frontal lobe. The spatial resolution of this model is relatively low, but the general locations agree with the fMRI data. The model was used as a spatial filter to derive the activation time-course of each regional source (source waveform) for the three deviant conditions in the grand average (Fig. 6) and the peak amplitudes in each individual separately (Fig. 7, left).

In both EEG and fMRI data, the response magnitudes from sites in the temporal lobes increased with deviance magnitude, whereas the responses from frontal sites were not modulated by the deviance magnitude across participants ( $F_{2,11} > 30$ ,  $P < 0.0001$  for effects of response origin, deviance magnitude, and their interaction; post hoc tests for deviance dependence of temporal sites  $P < 0.001$ , and frontal sites  $P = 0.89$ ; Fig. 7). Activity of the frontal sites showed in some individuals a trend toward increasing or decreasing responses with deviance mag-

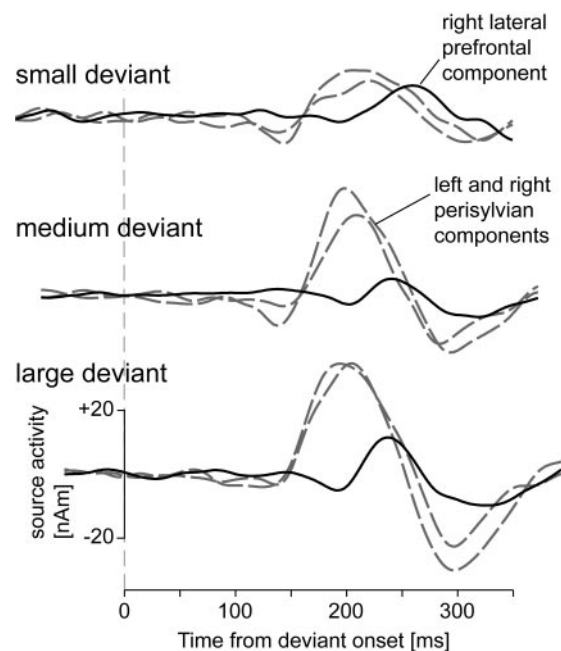


FIG. 6. Activation time-courses obtained from equivalent current dipole model of grand-average EEG responses to 3 deviants. Responses from bilateral temporal sources strongly depend on deviance magnitude. They are followed  $\sim 50$  ms later by response from right frontal source that is independent of deviance magnitude.

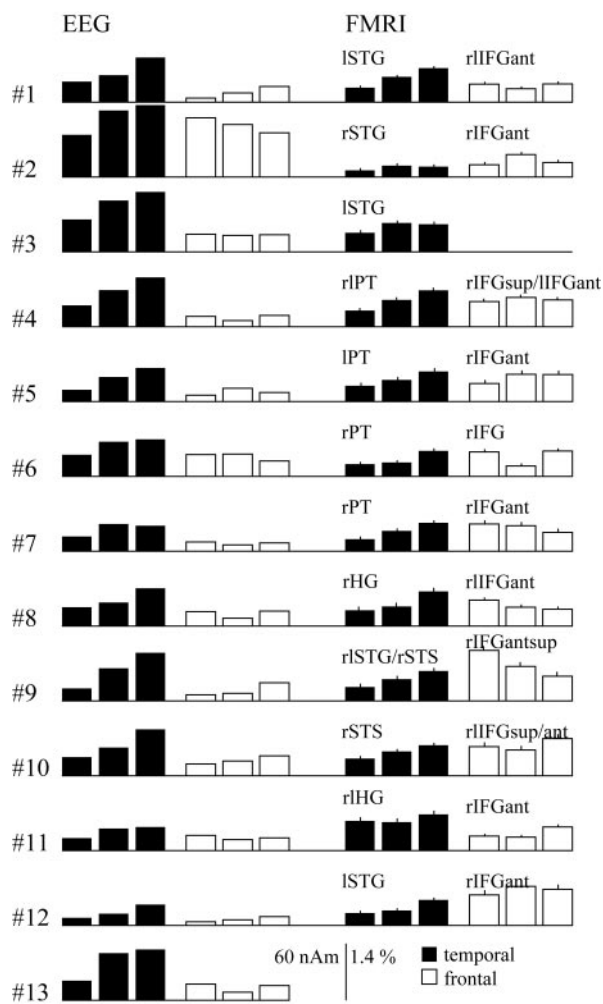


FIG. 7. Comparison of individual temporal lobe (black bars) and frontal lobe (white bars) responses between EEG and fMRI sessions. For clarity, only fMRI activity of local maximum that showed closest correlation with EEG responses is shown. r/l, right/left side structure.

nitude. Of the responsive sites in the temporal lobes, in 9 of 12 participants, the posterior STG and neighboring lateral PT showed the clearest modulation by deviance magnitude.

## DISCUSSION

Using an experimental design that overcomes previous methodical difficulties, we were able to localize the cerebral sites involved in the detection of duration changes in a constant stream of acoustic stimuli with greater precision than previously achieved. We characterized the degree of interindividual variability and showed, at the level of individual brains, different response patterns of temporal and frontal sites in the high-density EEG and fMRI data.

Responses in the temporal lobes were found in lateral and medial portions of HG, in the medial and lateral PT bordering HG, and along STG and STS, mostly posterior to HG.

In earlier brain imaging studies on preattentive auditory deviance detection, activation of the STG has been the most consistent finding (Doeller et al. 2003; Liebenthal et al. 2003; Mathiak et al. 2002; Molholm et al. 2005; Muller et al. 2002; Opitz et al. 1999, 2002; Rinne et al. 2005; Schall et al. 2003;

Tervaniemi et al. 2000, 2006). The region responsive to deviants in our study encroached the PT, mostly adjacent to STG, STS, and the medial and lateral parts of HG. The posterior STG and adjacent parts of the planum temporale showed an increase in activity with increasing deviance magnitude. Several anatomical areas have recently been delimited on the STG using observer-independent measures of differences in cyto- and receptoarchitecture (Morosan et al. 2005; Schleicher et al. 2005). According to this schema, area Te3 covers the posterior two thirds of the outer convexity of the STG (a posterior portion of Brodmann area 22). Its location fits well with the activated regions of STG that showed the highest dependence on deviance magnitude. Homolog regions in the primate auditory cortex belong to the parabelt, a tertiary region in the processing hierarchy of the auditory cortex (Kaas and Hackett 2000) that receives indirect connections from the primary auditory cortex through adjacent secondary (belt) areas (Kaas and Hackett 1998). In humans, the belt region would occupy the lateral HG and parts of the PT and planum polare adjacent to HG (Galaburda and Sanides 1980). We indeed found responses to the deviant sounds in the lateral HG and the planum temporale.

Medial portions of HG were found active in 6 (9 if responses slightly below statistical significance are included) of 12 participants. This suggests a contribution of the primary auditory cortex to deviance detection, which is in agreement with the demonstration of stimulus-specific adaptation of responses in the primary auditory cortex—a candidate neural correlate for some of the change responses observed in humans (Ulanovsky et al. 2003). Recordings of duration–MMN responses from depth electrodes in human HG also implicate the primary auditory cortex in change detection (unpublished observations). Opitz et al. (2005) showed that, during detection of frequency deviants, secondary areas on lateral HG seem to mediate a memory-trace based mismatch response, whereas activity on medial HG is related to a sensory mechanism of change detection, the stimulation of nonrefractory portions of tonotopic auditory cortex. The authors concluded that both of these mechanisms contribute to the MMN evoked by frequency deviants. It is unclear whether a similar sensory mechanism can account for the activation of primary auditory cortex during the detection of duration deviants. In mammals, duration-selective neurons have been found in the mouse inferior colliculus (Brand et al. 2000) and cat auditory cortex (He et al. 1997), but there is no indication of a large-scale topographic representation of sound duration in the human primary auditory cortex.

Based on these findings, we suggest that changes in the acoustic environment are initially detected at or below the level of the primary auditory cortex. Because the responses from the posterior STG and lateral PT follow the deviance magnitude most closely, these structures might extract the details of the acoustic change. The STS may be involved in a secondary process that is only loosely dependent on deviance magnitude and relies on input from the STG. There is indeed evidence that activity in the STS is more dependent on involuntary shifts of attention toward the deviant sound than on passive detection of the deviant (Sabri et al. 2006). Interestingly, the hemispheric distribution of the responses to duration changes might depend on the nature of the stimulus. In this study, we found no significant systematic differences in the responses from the left

and right superior temporal plane, whereas Tervaniemi et al. (2006) showed that complex speech- and music-like stimuli might evoke stronger responses in the left and right STG/STS, respectively.

In the majority of the participants, the responses in the IFG were found between the ascending and horizontal ramus. This region of the mid-ventrolateral prefrontal cortex corresponds to Brodmann area 45 (Amunts et al. 1999) and is connected with the STG and STS through the arcuate and superior longitudinal fascicle (Geschwind 1970; Petrides and Pandya 2002). There was a latency difference of ~50 ms between the peak in activity of the frontal and temporal sources in our equivalent current dipole model of the EEG responses. Tse et al. (2006) found a similar latency difference of ~60 ms with optical imaging in humans between activity in the superior temporal and inferior frontal lobe. These differences in the latency of temporal and frontal responses suggest that change-related activity in the IFG relies on afferent projections from the perisylvian region of the temporal lobes. Moreover, the latency difference was almost an order of magnitude higher than the passive conduction time between the two sites, suggesting that the activity observed in the mid-ventrolateral prefrontal cortex indicates cerebral processing rather than passive conduction. This processing is thought to relate to a possible switch of attention to the deviant sound (Giard et al. 1990). The P3a (Squires et al. 1975) is an event-related potential, probably generated in the prefrontal cortex (Knight 1984) and thought to indicate the allocation of attentional resources to novel events (Daffner et al. 2000; Escera et al. 1998). The latency of the frontal source (just between MMN and P3a) and its independence of deviance magnitude (whereas MMN and P3a increase in amplitude with deviance magnitude (Näätänen et al. 2004; Schröger and Wolff 1998) suggest that activity of the frontal source might indicate an intermediate step, perhaps a decision whether the stimulus is sufficiently novel to require attentional resources. Our deviant sounds are presented 85 times each and probably cease to be novel to the participants after the first few presentations. Because novelty is not an attribute of the stimulus, but an evaluation that arises in the brain of the listener, it must have a neural correlate. While the detection of a deviating sound can be based on sensory memory (which decays within a few seconds; Mäntysalo and Näätänen 1987; Sams et al. 1993), the decision of whether this sound is in fact novel (was not heard previously during the experiment) would have to be based on a process with a longer lasting memory span than the MMN system. An involvement of the right mid-ventrolateral prefrontal cortex (Brodmann areas 45 and 47/12) in such memory-based decisions has been shown in humans and macaque monkeys (Petrides 2005). Petrides et al. (2002) found activation of the mid-ventrolateral prefrontal cortex when human participants had to find a novel stimulus in pairs of familiar and novel visual stimuli. Activation in the perisylvian areas of the temporal lobe related to the detection of a deviant stimulus may trigger activity in the mid-ventrolateral prefrontal cortex to quickly determine whether the deviant stimulus requires additional attentional resources (call for attention; Öhman 1979). However, at least one study found frontal activity preceding activation in the temporal lobes by ~20 ms (Yago et al. 2001). According to these authors, the early frontal activity might reflect either a genuine MMN component, a frontal subcomponent of the N1 involved in the processing of

the frequency deviants presented, or an artifact of the procedure. Nevertheless, because activity in temporal and frontal regions largely overlaps in time, it is possible that one response is not merely triggered by the other but that information is flowing back and forth between these areas.

In summary, our results suggest that at least three regions of the cerebral cortex are involved in the automatic processing of acoustic changes: the primary auditory cortex, the posterior superior temporal gyrus and planum temporale, and the mid-ventrolateral prefrontal cortex. Analysis of the timing of activity in the EEG data and comparison with previous results support a hierarchical model in which these three regions are involved in the initial detection of an acoustical change, a detailed analysis of the change, and judgment of sufficient novelty for the allocation of attentional resources, respectively.

#### ACKNOWLEDGMENTS

We thank E. Brattico for helpful discussions throughout the study, K. Alho for comments on the manuscript, and A. Tarkiainen and M. Kattelus for technical assistance with the scanner.

#### GRANTS

This work was supported by Academy of Finland, National Centre of Excellence Program Grants 211486, 211487, 211488, and 213933.

#### REFERENCES

- Alain C, Woods DL, Knight RT. A distributed cortical network for auditory sensory memory in humans. *Brain Res* 812: 23–37, 1998.
- Alho K, Woods DL, Algazi A, Knight RT, Naatanen R. Lesions of frontal cortex diminish the auditory mismatch negativity. *Electroencephalogr Clin Neurophysiol* 91: 353–362, 1994.
- Amunts K, Schleicher A, Burgel U, Mohlberg H, Uylings HB, Zilles K. Broca's region revisited: cytoarchitecture and intersubject variability. *J Comp Neurol* 412: 319–341, 1999.
- Anwander A, Tittgemeyer M, von Cramon DY, Friederici AD, Knösche TR. Connectivity-based parcellation of Broca's area. *Cereb Cortex* In press.
- Brand A, Urban R, Grothe B. Duration tuning in the mouse auditory midbrain. *J Neurophysiol* 84: 1790–1799, 2000.
- Daffner KR, Mesulam MM, Scinto LF, Acar D, Calvo V, Faust R, Chabrier A, Kennedy B, Holcomb P. The central role of the prefrontal cortex in directing attention to novel events. *Brain* 123: 927–939, 2000.
- Doeller CF, Opitz B, Mecklinger A, Krick C, Reith W, Schröger E. Prefrontal cortex involvement in preattentive auditory deviance detection: neuroimaging and electrophysiological evidence. *Neuroimage* 20: 1270–1282, 2003.
- Edmister WB, Talavage TM, Ledden PJ, Weisskoff RM. Improved auditory cortex imaging using clustered volume acquisitions. *Hum Brain Mapp* 7: 89–97, 1999.
- Escera C, Alho K, Winkler I, Näätänen R. Neural mechanisms of involuntary attention to acoustic novelty and change. *J Cogn Neurosci* 10: 590–604, 1998.
- Galaburda A, Sanides F. Cytoarchitectonic organization of the human auditory cortex. *J Comp Neurol* 190: 597–610, 1980.
- Geschwind N. The organization of language and the brain. *Science* 170: 940–944, 1970.
- Giard MH, Perrin F, Pernier J, Bouchet P. Brain generators implicated in the processing of auditory stimulus deviance: a topographic event-related potential study. *Psychophysiology* 27: 627–640, 1990.
- Hall DA, Haggard MP, Akeroyd MA, Palmer AR, Summerfield AQ, Elliott MR, Gurney EM, Bowtell RW. "Sparse" temporal sampling in auditory fMRI. *Hum Brain Mapp* 7: 213–223, 1999.
- Haenschel C, Vernon DJ, Dwivedi P, Gruzeller JH, Baldeweg T. Event-related brain potential correlates of human auditory sensory memory-trace formation. *J Neurosci* 25: 10494–10501, 2005.
- He J, Hashikawa T, Ojima H, Kinouchi Y. Temporal integration and duration tuning in the dorsal zone of cat auditory cortex. *J Neurosci* 17: 2615–2625, 1997.
- Jasper H. Report of the committee on methods of clinical examination in electroencephalography: 1957. *Electroencephalogr Clin Neurophysiol* 10: 370–375, 1958.



- Kaas JH, Hackett TA.** Subdivisions of auditory cortex and levels of processing in primates. *Audiol Neurootol* 3: 73–85, 1998.
- Kaas JH, Hackett TA.** Subdivisions of auditory cortex and processing streams in primates. *Proc Natl Acad Sci USA* 97: 11793–11799, 2000.
- Knight RT.** Decreased response to novel stimuli after prefrontal lesions in man. *Electroencephalogr Clin Neurophysiol* 59: 9–20, 1984.
- Kujala T, Tervaniemi M, Schroger E.** The mismatch negativity in cognitive and clinical neuroscience: Theoretical and methodological considerations. *Biol Psychol* 74: 1–19, 2007.
- Liebenthal E, Ellingson ML, Spanaki MV, Prieto TE, Ropella KM, Binder JR.** Simultaneous ERP and fMRI of the auditory cortex in a passive oddball paradigm. *Neuroimage* 19: 1395–1404, 2003.
- Mäntysalo S, Näätänen R.** The duration of a neuronal trace of an auditory stimulus as indicated by event-related potentials. *Biol Psychol* 24: 183–195, 1987.
- Marco-Pallares J, Grau C, Ruffini G.** Combined ICA-LORETA analysis of mismatch negativity. *Neuroimage* 25: 471–477, 2005.
- Mathiak K, Rapp A, Kircher TT, Grodd W, Hertrich I, Weiskopf N, Lutzenberger W, Ackermann H.** Mismatch responses to randomized gradient switching noise as reflected by fMRI and whole-head magnetoencephalography. *Hum Brain Mapp* 16: 190–195, 2002.
- Molholm S, Martinez A, Ritter W, Javitt DC, Foxe JJ.** The neural circuitry of pre-attentive auditory change-detection: an fMRI study of pitch and duration mismatch negativity generators. *Cereb Cortex* 15: 545–551, 2005.
- Morosan P, Schleicher A, Amunts K, Zilles K.** Multimodal architectonic mapping of human superior temporal gyrus. *Anat Embryol (Berl)* 210: 401–406, 2005.
- Muller BW, Juptner M, Jentzen W, Muller SP.** Cortical activation to auditory mismatch elicited by frequency deviant and complex novel sounds: a PET study. *Neuroimage* 17: 231–239, 2002.
- Näätänen R.** The mismatch negativity: a powerful tool for cognitive neuroscience. *Ear Hear* 16: 6–18, 1995.
- Näätänen R.** Mismatch negativity: clinical research and possible applications. *Int J Psychophysiol* 48: 179–188, 2003.
- Näätänen R, Gaillard AW, Mäntysalo S.** Early selective-attention effect on evoked potential reinterpreted. *Acta Psychol (Amst)* 42: 313–329, 1978.
- Näätänen R, Pakarinen S, Rinne T, Takegata R.** The mismatch negativity (MMN): towards the optimal paradigm. *Clin Neurophysiol* 115: 140–144, 2004.
- Öhman A.** The orienting response, attention and learning: an information-processing perspective. In: *The Orienting Reflex in Humans*, edited by Kimmel HD, van Olst EH, Orlebeke JF. Hillsdale, NJ: Lawrence Erlbaum Associates, 1979, p. 443–471.
- Opitz B, Mecklinger A, Von Cramon DY, Kruggel F.** Combining electrophysiological and hemodynamic measures of the auditory oddball. *Psychophysiology* 36: 142–147, 1999.
- Opitz B, Rinne T, Mecklinger A, von Cramon DY, Schröger E.** Differential contribution of frontal and temporal cortices to auditory change detection: fMRI and ERP results. *Neuroimage* 15: 167–174, 2002.
- Opitz B, Schroger E, von Cramon DY.** Sensory and cognitive mechanisms for preattentive change detection in auditory cortex. *Eur J Neurosci* 21: 531–535, 2005.
- Paavilainen P, Simola J, Jaramillo M, Näätänen R, Winkler I.** Preattentive extraction of abstract feature conjunctions from auditory stimulation as reflected by the mismatch negativity (MMN). *Psychophysiology* 38: 359–365, 2001.
- Pantev C, Hoke M, Lehnertz K, Lutkenhoner B.** Neuromagnetic evidence of an amplipic organization of the human auditory cortex. *Electroencephalogr Clin Neurophysiol* 72: 225–231, 1989.
- Petrides M.** Lateral prefrontal cortex: architectonic and functional organization. *Philos Trans R Soc Lond B Biol Sci* 360: 781–795, 2005.
- Petrides M, Alivisatos B, Frey S.** Differential activation of the human orbital, mid-ventrolateral, and mid-dorsolateral prefrontal cortex during the processing of visual stimuli. *Proc Natl Acad Sci USA* 99: 5649–5654, 2002.
- Petrides M, Pandya DN.** Comparative cytoarchitectonic analysis of the human and the macaque ventrolateral prefrontal cortex and corticocortical connection patterns in the monkey. *Eur J Neurosci* 16: 291–310, 2002.
- Pulvermüller F, Shtyrov Y, Ilmoniemi RJ, Marslen-Wilson WD.** Tracking speech comprehension in space and time. *Neuroimage* 31: 1297–1305, 2006.
- Rinne T, Degerman A, Alho K.** Superior temporal and inferior frontal cortices are activated by infrequent sound duration decrements: an fMRI study. *Neuroimage* 26: 66–72, 2005.
- Sabri M, Liebenthal E, Waldron EJ, Medler DA, Binder JR.** Attentional modulation in the detection of irrelevant deviance: a simultaneous ERP/fMRI study. *J Cogn Neurosci* 18: 689–700, 2006.
- Sams M, Hari R, Rif J, Knuutila J.** The human auditory sensory memory trace persists about 10 sec—neuromagnetic evidence. *J Cogn Neurosci* 5: 363–370, 1993.
- Schall U, Johnston P, Todd J, Ward PB, Michie PT.** Functional neuroanatomy of auditory mismatch processing: an event-related fMRI study of duration-deviant oddballs. *Neuroimage* 20: 729–736, 2003.
- Schleicher A, Palomero-Gallagher N, Morosan P, Eickhoff SB, Kowalski T, de Vos K, Amunts K, Zilles K.** Quantitative architectural analysis: a new approach to cortical mapping. *Anat Embryol (Berl)* 210: 373–386, 2005.
- Schröger E, Wolff C.** Behavioral and electrophysiological effects of task-irrelevant sound change: a new distraction paradigm. *Brain Res Cogn Brain Res* 7: 71–87, 1998.
- Sharbrough F, Chatrian G, Lesser RP, Lüders H, Nuwer M, Picton T.** American Electroencephalographic Society guidelines for standard electrode position nomenclature. *J Clin Neurophysiol* 8: 200–202, 1991.
- Shestakova A, Brattico E, Soloviev A, Klucharev V, Huotilainen M.** Orderly cortical representation of vowel categories presented by multiple exemplars. *Brain Res Cogn Brain Res* 21: 342–350, 2004.
- Squires NK, Squires KC, Hillyard SA.** Two varieties of long-latency positive waves evoked by unpredictable auditory stimuli in man. *Electroencephalogr Clin Neurophysiol* 38: 387–401, 1975.
- Tervaniemi M, Medvedev SV, Alho K, Pakhomov SV, Roudas MS, Van Zuijen TL, Näätänen R.** Lateralized automatic auditory processing of phonetic versus musical information: a PET study. *Hum Brain Mapp* 10: 74–79, 2000.
- Tervaniemi M, Szameitat AJ, Kruck S, Schröger E, Alter K, De Baene W, Friederici AD.** From air oscillations to music and speech: functional magnetic resonance imaging evidence for fine-tuned neural networks in audition. *J Neurosci* 26: 8647–8652, 2006.
- Tse CY, Tien KR, Penney TB.** Event-related optical imaging reveals the temporal dynamics of right temporal and frontal cortex activation in pre-attentive change detection. *Neuroimage* 29: 314–320, 2006.
- Ulanovsky N, Las L, Nelken I.** Processing of low-probability sounds by cortical neurons. *Nat Neurosci* 6: 391–398, 2003.
- Worsley KJ, Liao CH, Aston J, Petre V, Duncan GH, Morales F, Evans AC.** A general statistical analysis for fMRI data. *Neuroimage* 15: 1–15, 2002.
- Yago E, Escera C, Alho K, Giard MH.** Cerebral mechanisms underlying orienting of attention towards auditory frequency changes. *Neuroreport* 12: 2583–2587, 2001.